Response dynamics of the frequency comb output from a femtosecond fiber laser

B. R. Washburn, W. C. Swann, and N. R. Newbury

National Institute of Standards and Technology, 325 Broadway, Boulder, CO 80305
nnewbury@boulder.nist.gov

Abstract: The frequency comb from a mode-locked fiber laser can be stabilized through feedback to the pump power. An understanding of the mechanisms and bandwidth governing this feedback is of practical importance for frequency comb design and of basic interest since it provides insight into the rich nonlinear laser dynamics. We compare experimental measurements of the response of a fiber-laser frequency comb to theory. The laser response to a pump-power change follows that of a simple low-pass filter with a time constant set by the gain relaxation time and the system-dependent nonlinear loss. Five different effects contribute to the magnitude of the response of the frequency comb spacing and offset frequency but the dominant effects are from the resonant contribution to the group velocity and intensity-dependent spectral shifts. The origins of the intensity-dependent spectral shifts are explained in terms of the laser parameters.

Work of an agency of the U.S. government; not subject to copyright.

OCIS codes: (140.3510) Lasers, Fiber; (190.4370) Nonlinear Optics, Fibers; (120.3930) Metrological Instrumentation;

References and links

1. B. R. Washburn, S. A. Diddams, N. R. Newbury, J. W. Nicholson, M. F. Yan, and C. G. Jørgensen, "Phase-locked erbium-fiber-laser-based frequency comb in the near infrared," Opt. Lett. **29**, 250-252 (2004).
2. T. R. Schibili, K. Minoshima, F.-L. Hong, H. Inaba, A. Onae, H. Matsumoto, I. Hartl, and M. N. Fermann, "Frequency metrology with a turnkey all-fiber system," Opt. Lett. **29**, 2467-2469 (2004).
3. P. Kubina, P. Adel, F. Adler, G. Grosche, T. W. Hänsch, R. Holzwarth, A. Leitenstorfer, B. Lipphardt, and H. Schnatz, "Long term comparison of two fiber based frequency comb systems," Opt. Express **13**, 904-909 (2005) http://www.opticsexpress.org/abstract.cfm?URI=OPEX-13-3-904.
4. E. Benkler, H. R. Telle, A. Zach, and F. Tauser, "Circumvention of noise contributions in fiber laser based frequency combs," Opt. Express **13**, 5662-5668 (2005), http://www.opticsexpress.org/abstract.cfm?URI=OPEX-13-15-5662.
5. S. A. Diddams, D. J. Jones, S. T. C. J. Ye, J. L. Hall, J. K. Ranka, R. S. Windeler, R. Holzwarth, T. Udem, and T. W. Hansch, "Direct Link between Microwave and Optical Frequencies with a 300 THz Femtosecond Laser Comb," Phys. Rev. Lett. **84**, 5102 (2000).
6. N. R. Newbury and B. R. Washburn, "Theory of the frequency comb output from a femtosecond fiber laser," IEEE J. of Quantum Electron. **41**, 1388-1402 (2005).
7. H. A. Haus and A. Mecozzi, "Noise of mode-locked lasers," IEEE J. Quantum Electron. **29**, 983-996 (1993).
8. L. Xu, C. Spielmann, A. Poppe, T. Brabec, F. Krausz, and T. W. Hänsch, "Route to phase control of ultrashort light pulses," Opt. Lett. **21**, 2008-2010 (1996).
9. F. W. Helbing, G. Steinmeyer, U. Keller, R. S. Windeler, J. Stenger, and H. R. Telle, "Carrier-envelope offset dynamics of mode-locked lasers," Opt. Lett. **27**, 194-196 (2002).
10. K. W. Holman, R. J. Jones, A. Marian, S. T. Cundiff, and J. Ye, "Intensity-related dynamics of femtosecond frequency combs," Opt. Lett. **28**, 851-853 (2003).
11. H. A. Haus and E. P. Ippen, "Group velocity of solitons," Opt. Lett. **26**, 1654-1656 (2001).
12. N. Haverkamp, H. Hundertmark, C. Fallnich, and H. R. Telle, "Frequency stabilization of mode-locked Erbium fiber lasers using pump power control," Appl. Phys. B **78**, 321-324 (2004).
13. B. R. Washburn, R. Fox, N. R. Newbury, J. W. Nicholson, K. Feder, P. S. Westbrook, and C. G. Jørgensen, "Fiber-laser-based frequency comb with a tunable repetition rate," Opt. Express **12**, 4999-5004 (2004), http://www.opticsexpress.org/abstract.cfm?URI=OPEX-12-20-4999.
14. K. Tamura, H. A. Haus, and E. P. Ippen, "Self-starting additive pulse mode-locked erbium fiber ring laser," Electron. Lett. **28**, 2226-7 (1992).

#9471 - $15.00 USD Received 10 November 2005; revised 6 December 2005; accepted 13 December 2005
(C) 2005 OSA

15. J. W. Nicholson, P. S. Westbrook, K. S. Feder, and A. D. Yablon, "Supercontinuum generation in UV irradiated fibers," Opt. Lett. **29**, 2363-2365 (2004).
16. J. Rauschenberger, T. M. Fortier, D. J. Jones, J. Ye, and S. T. Cundiff, "Control of the frequency comb from a mode-locked Erbium-doped fiber laser," Opt. Express **10**, 1404-1410 (2002), http://www.opticsexpress.org/abstract.cfm?URI=OPEX-10-24-1404.
17. L. E. Nelson, D. J. Jones, K. Tamura, H. A. Haus, and E. P. Ippen, "Ultrashort-pulse fiber ring lasers," Appl. Phys. B **65**, 277-94 (1997).
18. J. D. Moores, "On the Ginzburg-Landau laser mode-locking model with fifth-order saturable absorber term," Opt. Commun. **96**, 65-70 (1993).
19. B. R. Washburn, S. Diddams, N. R. Newbury, J. W. Nicholson, M. F. Yan, and C. G. Jørgensen, "A phase locked, fiber laser-based frequency comb: limit on optical linewidth," in *Proceedings of Conference on lasers and Electro-optics*, (Optical Society of America, 2004)
20. E. Desurvire, *Erbium-Doped Fiber Amplifiers*. (Wiley, New York, 1994).
21. V. S. Grigoryan, T. Yu, E. A. Golovchenko, C. R. Menyuk, and A. N. Pilipetskii, "Disperison-managed soliton dynamics," Opt. Lett. **22**, 1609-1611 (1997).
22. S. M. J. Kelly,"Characteristic sideband instability of periodically amplified average soliton," Electron. Lett. **28**, 806-807 (1992).

1. Introduction

Mode-locked fiber lasers are a compact, potentially turn-key frequency comb source for optical frequency metrology and other applications [1-4]. The mode-locked laser outputs a pulse train in the time domain, which results in a frequency comb in the frequency domain. The comb spacing is the laser's repetition rate, f_r, and the comb offset from zero frequency is the carrier-envelope offset (CEO) frequency, f_{CEO}. By phase-locking f_r and f_{CEO} to a stable rf or optical frequency, the resulting comb can be used as an infrared spectral ruler for measuring optical frequencies [5]. So far, work on phase-locked fiber-laser frequency combs has been mainly experimental, so the question remains as to what mechanisms determine the magnitude and bandwidth of the response of the comb parameters, f_r and f_{CEO}, to a change in laser pump power. A recently developed theory [6] describes the response of f_r and f_{CEO} to changes in the laser's operating parameters, starting with the Master equation [7] and including the resonant contribution to the index of refraction from the gain medium, third-order dispersion (TOD), stimulated Raman scattering (SRS), frequency-dependent loss, self-phase modulation (SPM), self-steepening (SS), spectral shifts, and saturation of the self-amplitude modulation (SAM). Here we present experimental measurements of the response of a fiber-laser frequency comb to changes in the pump power, finding good agreement with theory.

There are some similarities between the response of the fiber-laser frequency comb and Ti:Sapphire laser-based frequency combs using externally broadening in microstructure fiber, where previous work has focused on the effects of SS, SPM (or the Kerr phase shift), and empirically observed spectral shifts [6, 8-11]. The effects of SS and SPM also appear for a fiber-laser frequency comb but are of less significance. Pump-induced spectral shifts remain important for a fiber-laser frequency comb [12]; here we explain their origin. Also, unlike the Ti:Sapphire laser-based combs, the fiber laser-based frequency comb has a pronounced limited response bandwidth. Here we discuss this bandwidth and its implications for a low-noise comb.

A number of physical mechanisms, which are described quantitatively in [6], can lead to pump-induced changes in the repetition frequency and offset frequency of the comb. For a given frequency comb system, the dominant mechanism(s) will depend on the particular system parameters. For the fiber laser-based frequency comb analyzed here we find the dominant mechanisms are the resonant gain contribution and spectral shifts with smaller contributions from third-order dispersion and self-steepening. The theory of Ref. [6] and the experimental approach followed here are reasonably general and could be used to identify the dominant mechanisms for frequency combs based on other fiber lasers or on entirely different laser systems, such as Ti:Sapphire lasers.

We first briefly describe the frequency comb used in this experiment. We then discuss the basic laser response bandwidth, the magnitude of the response of f_{CEO}, the magnitude of the

#9471 - $15.00 USD Received 10 November 2005; revised 6 December 2005; accepted 13 December 2005
(C) 2005 OSA

response of f_r, and finally the intensity-dependent spectral shifts. In each section, we briefly review the relevant aspects of the underlying theory, provide the experimental results and compare these results to the theoretical predictions.

2. Frequency comb generation from a mode-locked fiber laser

The data were mainly acquired using a frequency comb produced by a ring laser [13, 14], shown in Fig. 1(a), figure-eight design can also be employed and was also used in measurements of the laser response bandwidth [1]. In the frequency domain, the laser output forms a frequency comb with offset frequency, f_{CEO}, and spacing, f_r. The f_{CEO} was detected using supercontinuum generation [15] followed by a collinear f-to-2f interferometer, [2] while f_r was detected by simply directing the laser output to a photodiode. To stabilize the comb, f_{CEO} and f_r were phase-locked to a reference through feedback to the pump power and the cavity length, respectively. However, for most of these measurements, the comb was free-running. In the work reported here, we focused on the effects of pump-power modulation on the comb; however, similar measurements taken modulating the cavity length also show good agreement with theory.

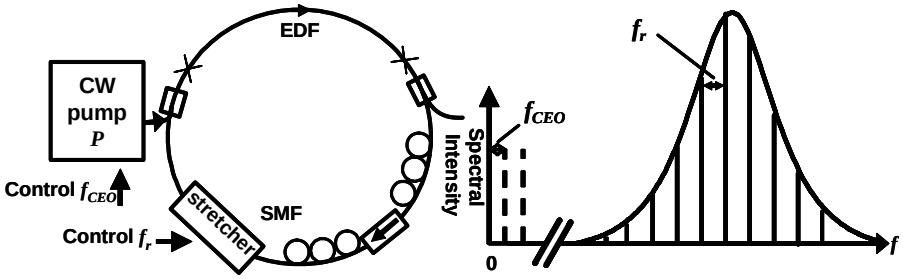

Fig. 1. A schematic of the fiber ring laser. The laser consisted of 1 m of Erbium doped fiber (EDF) that was pumped with a 980 nm diode, and 3 m of single-mode fiber with a net anomalous dispersion of -0.06 ps^2. Self-amplitude modulation is provided by a polarizer/isolator combination that is sandwiched between two polarization controllers.

3. Response bandwidth of the fiber laser system

The offset frequency, f_{CEO}, is typically phase-locked to an rf reference by feeding back to the pump power. In any feedback system, a large feedback bandwidth is preferred; however, the observed feedback bandwidth to the pump power is limited to the kHz range [1, 12, 16]. Therefore, one of the basic questions related to phase-locking a fiber laser is what limits this feedback bandwidth?

The time-dependence of the response of the laser to a pump power change is complicated due to the interplay of the slow gain dynamics in the Erbium doped fiber (EDF) and the much faster laser dynamics. Figure 2 shows the four main components comprising the mode-locked laser. The first three, a gain section, cavity loss, and self-amplitude modulation provide the necessary pulse energy-dependent gain for mode-locking. Because the Erbium gain has such a slow response time, gain saturation alone cannot stabilize the system against perturbations and it is necessary to include a fourth component in the cavity, namely the saturation of the self-amplitude modulation effect. This saturation is modeled as an energy-dependent loss and is physically manifested though the generation of Kelly sidebands or by the over-rotation of the nonlinear polarization rotation [6, 17, 18]. Saturation of the SAM provides stability by causing the net cavity gain to decrease with increasing pulse energy, corresponding to a negative slope of the net gain versus pulse energy as shown in Fig. 2(b). This negative slope is characterized by a nonlinear loss η [see Fig. 2(b)]. The greater the value of η, the greater the stability of the pulse train to perturbations. The value of η will be laser system-dependent.

#9471 - $15.00 USD Received 10 November 2005; revised 6 December 2005; accepted 13 December 2005
(C) 2005 OSA

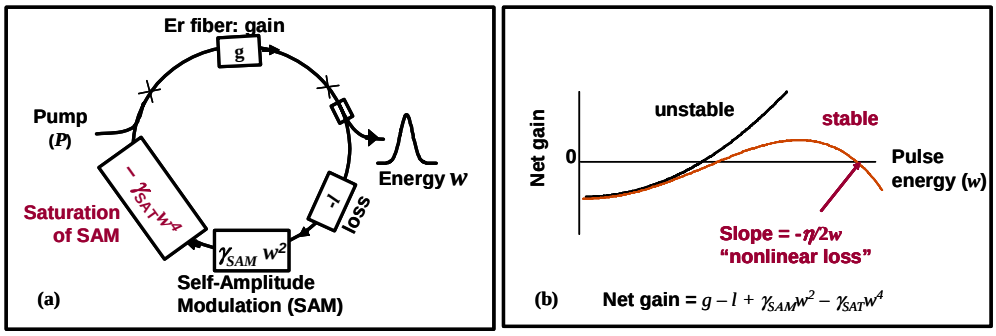

Fig. 2. (a) Schematic representation of the lumped gain, loss, and SAM experienced by the pulse electric field as it traverses the cavity. Saturation of the SAM is added to insure stability. Here it is convenient to describe the SAM and its saturation heuristically in terms of the pulse energy, w, and the two parameters γ_{SAM} and γ_{SAT}. In Ref. [6] a more rigorous treatment is given where the SAM and its saturation are described in terms of the electric field amplitude, which is proportional to w for a soliton, and a pair of parameters. (b) Without saturation of the SAM (and without gain saturation), the system is unstable to pulse energy perturbations (black line). Inclusion of SAM saturation leads to a stable solution (red line). In terms of the variables in Fig. 2(a), $\eta = 4\,(g\text{-}l) + 4\gamma_{SAT}w^4$.

Over longer timescales, an increase in pulse energy, w, does cause the gain, g, to relax to a new, lower value due to increased gain saturation by the circulating signal power. For a gain relaxation time of T_g and a round-trip time of T_r, the evolution with time T of perturbations to the pulse energy, Δw, and gain, Δg, are given by [6],

$$\begin{aligned} \partial_T \Delta w &= -\frac{1}{T_r}\left[\eta \Delta w - 2\Delta g\, w\right], \\ \partial_T \Delta g &= -\frac{1}{T_g}\left[\Delta g + g_w \frac{\Delta w}{w} - g_P \frac{\Delta P}{P}\right], \end{aligned} \tag{1}$$

where the first equation can be derived from Fig. 2 and the second equation describes the simple exponential decay of the gain to its steady state value where $g_w = -wdg/dw$ and $g_P = Pdg/dP$. For the high gain values encountered in a fiber laser, $g_w = g_P = 1/2$ (assuming P is measured from threshold) [6].

The solution to these equations is a simple exponential decay with a corresponding 3-dB bandwidth $\nu_{3\mathrm{dB}} = \left(1+\eta^{-1}\right)\nu_{3\mathrm{dB}}^{Er}$, where $\nu_{3\mathrm{dB}}^{Er} = 1/\left(2\pi T_g\right)$ is the response bandwidth of the gain section alone, which is dominated by stimulated transitions from the signal and pump beams rather than spontaneous emission. This bandwidth directly limits the available bandwidth for feeding back to the pump power to control the comb parameters.

From Eq. (1), the steady-state values for the changes in pulse energy and gain resulting from a change in pump power are $dw/dP = 2w\eta^{-1}\left(dg/dP\right)$ and $dg/dP = \left(\nu_{3\mathrm{dB}}^{Er}/\nu_{3\mathrm{dB}}\right)\times\left(2P\right)^{-1}$, defining $\Delta w/\Delta P = dw/dP$ and using $g_w = g_P = 1/2$. Note that $dg/dP \to 0$ for $\eta \to 0$ corresponding to the fact that the overall gain must equal the overall loss in the laser and if there is no pulse-energy dependent change in the overall loss, *i.e.* η=0, there can be none in the gain.

The theory predicts three important results. First, the response will follow a simple exponential decay rather than exhibit relaxation oscillations. Second, the laser response bandwidth will exceed that of the Erbium gain medium due to coupling with the laser dynamics. Third, the closer the bandwidth to the Erbium gain response (higher values of η), the greater the laser stability since any intrinsic fluctuations will be more strongly damped.

#9471 - $15.00 USD Received 10 November 2005; revised 6 December 2005; accepted 13 December 2005
(C) 2005 OSA

To verify these three predictions, we measured the response of a ring laser, a figure-eight laser, and a section of EDF that was pumped with identical pump and signal powers as in the laser cavities. To measure the response, we modulated the pump power and measured the output as a function of the modulation frequency using a standard swept-sine technique. The response of the Er gain medium was determined by temporarily "breaking open" the laser, so that it acted as a single-pass amplifier, injecting the appropriate amount of signal power, and measuring the modulation of the output power. The response of the lasers was monitored by measuring the output power, but separate measurements of the response of f_r, and f_{CEO} produced the same normalized response to the modulation. The results are given in Fig. 3(a). All three responses show a simple roll-off with frequency as in a low-pass filter. (At higher pump powers, a "bump" is sometimes observed in the laser response which we attribute to relaxation oscillations from cw-breakthrough as discussed later.) The 3-dB bandwidth of the Er gain in Fig. 3 is $\nu_{3\mathrm{dB}}^{Er} = 1.6$ kHz. The bandwidths of the lasers' response are larger at 4.2 kHz and 17 kHz for the figure-eight and ring laser respectively, corresponding to the physically reasonable values of $\eta \approx 1/1.6$ and $\eta \approx 1/10$.

Based on this bandwidth argument alone, one might expect better performance for systems with a lower value of η since it allows for a higher feedback bandwidth for phase-locking f_{CEO} to a reference. However, this higher performance may well not be achieved since the lower value of η also corresponds to the less stable system. Indeed, the width of the f_{CEO} beat was narrower for the lower-bandwidth system, as shown in Fig. 3(b). The f_{CEO} beat note, which exhibits a Lorentzian line shape, [19] has a width of 150 kHz for the 4.2 kHz-bandwidth figure-eight laser based comb and 1.4 MHz for the 17 kHz-bandwidth ring laser based comb. The lower stability of the ring laser is not necessarily attributable to a fundamental design difference with the figure-eight laser, but possibly to greater back reflections (losses) from the bulkhead fiber-to-fiber connectors used in this cavity that seed system instabilities. Since the noise on f_{CEO} is higher, the higher bandwidth afforded by the ring laser will not necessarily lead to a tighter phase-lock on f_{CEO}.

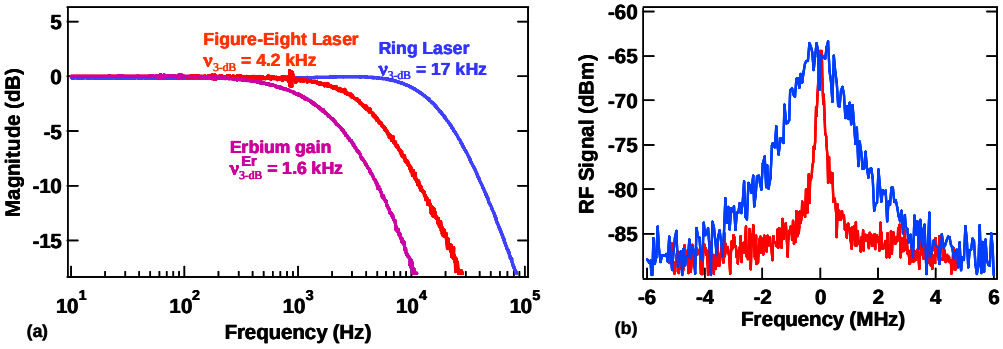

3. (a) Normalized response of the gain medium and two different lasers as a function of the modulation frequency of the pump power. The laser relaxation times are always greater than that of the Erbium gain medium. (b) Measured f_{CEO} beat note for the figure-eight laser (red) and the ring laser (blue).

4. Response of the offset frequency

The second important factor in understanding the phase-locking of the fiber-laser frequency comb is the magnitude of the response to a pump-power change. In this section, we discuss the magnitude of the change in the offset frequency with pump power as a function of the fundamental Kerr phase shift and of pump-induced shifts in the repetition frequency. The fundamental causes of the pump-induced shift of the repetition frequency are discussed in Section 5.

The offset frequency of the comb (see Fig. 1) is given by $f_{CEO} = f_r \varphi_{CEO}/(2\pi)$, where φ_{CEO} is the change in the carrier-envelope offset phase per pulse. (This quantity is sometimes denoted

#9471 - $15.00 USD Received 10 November 2005; revised 6 December 2005; accepted 13 December 2005
(C) 2005 OSA

$\Delta\varphi_{CEO}$ in other work, but here we follow the notation of Ref. [6] to avoid the otherwise cumbersome notation of $\Delta\Delta\varphi_{CEO}$ to describe perturbations to this quantity.) φ_{CEO} can change because of a shift in the pulse envelope arrival time or a shift in the carrier phase; a shift in pulse arrival time, ΔT_r, leads to a phase shift $\Delta\varphi_{CEO} = -\omega_c \Delta T_r$ where ω_c is the carrier frequency, and a shift in the nonlinear carrier phase, φ_{spm}, leads directly to a phase shift $\Delta\varphi_{CEO} = \Delta\varphi_{spm}$. The dominant causes of $\Delta\varphi_{CEO}$ are listed in Fig. 4(a).

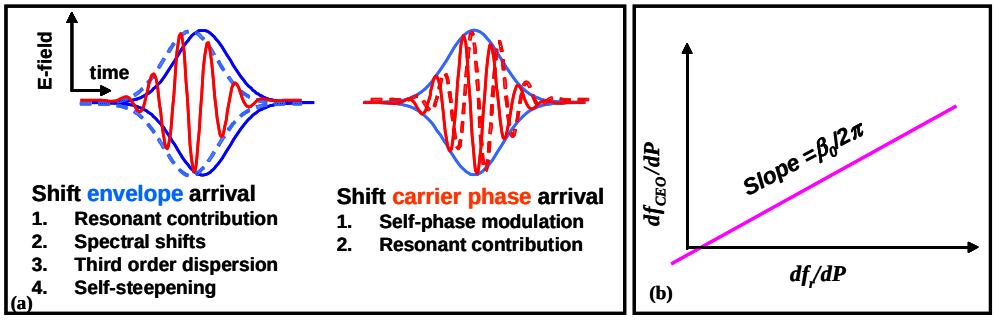

Fig. 4. (a) The different mechanisms contributing to the change in φ_{CEO}. Note that a spectral shift in the carrier frequency effectively enters only as a shift in the envelope arrival time. The four mechanisms contributing to changes in the envelope arrival time (*i.e.* repetition frequency) are discussed in more detail in Section 5. (b) The expected linear relationship between the response of the offset frequency and the repetition frequency from Eq. (2) .

The shift in f_{CEO} is complicated by the fact f_{CEO} is the product of φ_{CEO} and f_r; a shift in envelope arrival time will shift both φ_{CEO} as discussed above and directly shift f_r by $\Delta f_r = -f_r^2 \Delta T_r$. A careful treatment yields the following expression for the change in the CEO offset frequency versus pump power [6],

$$\frac{df_{CEO}}{dP} = \frac{\beta_0}{2\pi}\left(\frac{df_r}{dP}\right) + \frac{f_r}{2\pi}\left(\frac{d\varphi_{spm}}{dP}\right) \tag{2}$$

where $\beta_0 = nL\omega_0/c$ is the lumped, average fiber propagation constant for the laser of length L and average index of refraction n. The first term accounts for shifts in the carrier envelope arrival time and the second accounts for shifts in the carrier phase from self-phase modulation. Equation (2) predicts two important results [see Fig. 4(b)]. First, it predicts a linear relationship between df_{CEO}/dP and df_r/dP with a slope of $\beta_0/(2\pi)$. Second, it predicts an intercept given by the pump-induced change to the SPM, or Kerr, phase shift.

To measure the magnitude of the response of the comb parameters to a change in pump power, *e.g.* df_{CEO}/dP and df_r/dP, we applied a weak ~1 mW square-wave modulation to the pump power of the ring laser and monitored the resulting square-wave modulation of f_{CEO} and f_r using frequency counters. The modulation frequency was chosen to be ~0.5 Hz as a tradeoff between avoiding thermal effects (which do not play a part in phase-locking the comb) and achieving sufficient resolution on the frequency counters. Figure 5 shows an example of the resulting data.

Using this pump power modulation, values of df_{CEO}/dP and df_r/dP were determined for different laser polarizer settings and average pump powers. In Fig. 6, df_{CEO}/dP is plotted versus df_r/dP yielding a straight line with a fitted slope of 3.8×10^6, which corresponds to the predicted value of $\beta_0/2\pi = 3.9\times10^6$. The fitted intercept at $df_r/dP=0$ is df_{CEO}/dP = 0.4 MHz/mW, which should agree with the second term in Eq. (2). The phase shift for an autosoliton with zero chirp is $\varphi_{spm} = \delta A^2/2$, where δ is the lumped nonlinearity for the laser estimated to be 6 kW^{-1} and A^2 is the peak intensity estimated to be A^2= 0.07 nJ/230 fs = 0.3 kW. From the empirically measured pulse energy scaling (discussed later), we expect A^2 to scale as $P^{3/2}$. For our pump-power of ~40 mW, the predicted intercept is then

#9471 - $15.00 USD Received 10 November 2005; revised 6 December 2005; accepted 13 December 2005
(C) 2005 OSA

$f_r/(2\pi) \times (d\varphi_{spm}/dP) = 3f_r\varphi_{spm}/(4\pi P) = 0.25$ MHz/mW, which is only about half the fitted value. However, there is an added contribution to the intercept that is not included in the formal theory of Ref. [6] and derivation of Eq. (2), which assumed a Lorentzian gain profile. For a Lorentzian gain, there is no resonant contribution to β_0 (related to the phase velocity); there is only a resonant contribution to β_1 (related to the group velocity). However, the Erbium gain is not exactly Lorentzian in shape so that in general there will be a resonant gain contribution to β_0, and therefore to the carrier phase, that will shift with pump power. This shift will add to the intercept given in Eq. (2). For strong signal saturation, an exact calculation of this effect is difficult, but using existing data [20] it is of the correct order of magnitude to explain the discrepancy.

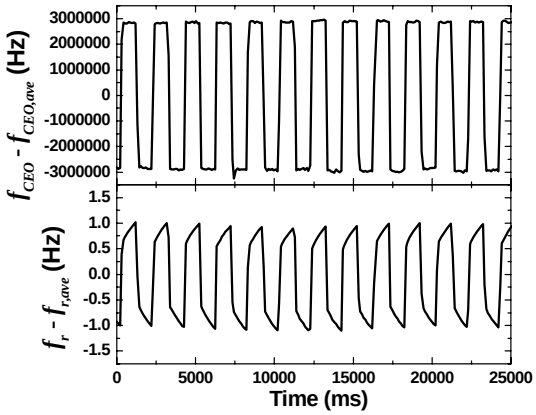

Fig. 5. Counted values of f_r and f_{CEO} for a 0.5 Hz square-wave modulation of the pump power. The slight slope on the f_r data is a result of thermal effects. The counter gate time was 100 ms. The average repetition rate was about 50 MHz.

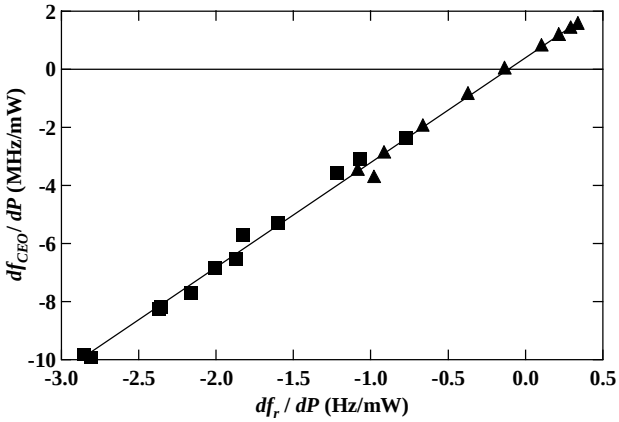

Fig. 6. The measured df_{CEO}/dP versus df_r/dP. The two symbols refer to data taken with different polarizer settings. For each polarizer setting, the data correspond to different pump powers. The solid line is a straight-line fit.

We have shown that the simple linear relationship of Eq. (2) can describe the relative changes in f_{CEO} and f_r to the pump power. This expression is one useful way to characterize the comb sensitivity. Another proven, useful representation of the comb sensitivity to control parameters (*i.e.* pump power or cavity length) is the "fixed point" [12]. A change in pump power will cause an expansion of the comb about a specific frequency value – the fixed point.

#9471 - $15.00 USD Received 10 November 2005; revised 6 December 2005; accepted 13 December 2005
(C) 2005 OSA

This fixed point is extracted from Fig. 6 as $f_{fix}=n_{fix}f_r - f_{CEO}$, where $n_{fix}=(df_{CEO}/dP)/(df_r/dP)$. If the first term in Eq. (2) dominates, then $n_{fix}=\beta_0/(2\pi)$ giving $2\pi f_{fix} = \beta_0 f_r - 2\pi f_{CEO} = \beta_0 f_r - f_r(\varphi_{spm}+\beta_0-\omega_0 T_r) = \omega_0 - f_r\varphi_{spm} \approx \omega_0$, using the fact that $\varphi_{CEO} = \varphi_{spm} + \beta_0 - \omega_0 T_r$ [6]. In other words, if the shift in the carrier envelope dominates then the fixed point is at the carrier frequency, i.e. $f_{fix} = \omega_0/2\pi$, regardless of whether the effect arises from TOD, gain dispersion, self-steepening, or spectral shifts.

5. Response of the repetition frequency

In the previous section, we found that the pump-induced change in the offset frequency is typically dominated by the pump-induced change in the repetition frequency, df_r/dP. So the next question to address is what are the fundamental reasons for a pump-induced change in the repetition frequency?

There are a number of perturbations that affect the round-trip time around the cavity, T_r, and therefore the repetition rate, f_r. The perturbations considered here, as listed in Fig. 4(a), are: resonant gain contribution, spectral shifts, third-order dispersion, and self-steepening. If one includes these perturbations the total round trip time is given by [6]

$$T_r = \frac{1}{f_r} = \beta_1 + \omega_\Delta \beta_2 + \frac{1}{2}\omega_{rms}^2 \beta_3 + \frac{g}{\Omega_g} + \frac{\mu A^2 \delta}{\omega_0} \tag{3}$$

where $\beta_n = d^n\beta / d\omega^n |_{\omega_0}$ are the frequency-derivatives of the lumped linear fiber propagation constant evaluated at the gain peak, ω_0. The first term is just the expected round-trip time for a group velocity of L/β_1. The second term is a correction due to spectral shifts $\omega_\Delta = \omega_c - \omega_0$ of the carrier from ω_0. The third term is a correction due to third-order dispersion, where ω_{rms} is the root-mean-square pulse spectral width, and we assume $\omega_{rms} >> \omega_\Delta$. The fourth term is the resonant contribution from the Erbium gain assuming a Lorentzian gain shape with peak value g and bandwidth Ω_g. The final term is the nonlinear self-steepening contribution, where μ=1.3 is a minor numerical correction related to the modal shape. (This final term is the effective contribution to β_1 from the SPM term in the nonlinear Schrödinger equation.)

A calculation of df_r/dP involves taking the derivative of each term on the right hand side of Eq. (3). The first term, β_1, vanishes since it is by definition the linear part of the propagation constant. The second term is proportional to the pump-induced spectral shift, $d\omega_\Delta/dP$, which can be measured experimentally as discussed in greater detail in Section 6. For the remaining terms, we relate the relevant derivatives (of ω_{rms}, g, and A^2) to the derivative of the pulse energy, dw/dP, and ultimately to the fractional change in the pump power in order to derive a more useful expression for df_r/dP. For a true soliton, the spectral width ω_{rms} scales linearly with pulse energy w, as is assumed in Ref. [6]. However, pulses that propagate around the ring laser are actually dispersion-managed (DM) solitons due to the alternating positive and negative dispersion (from the EDF and single-mode fiber) around the cavity. The scaling of ω_{rms} (and A) with w for a DM soliton should be weaker [21]. By taking spectra versus output pulse energy, we measured a scaling of $\omega_{rms} \propto w^{1/2}$. Similarly, although A scales linearly with w for a true soliton, there is a weaker scaling for the dispersion managed soliton; assuming zero chirp gives $A^2 \propto w\omega_{rms}$, so that A scales as $A \propto w^{3/4}$. Using the expression given in Section 3 for the pulse-energy dependence, $dw/dP=(1+\eta)^{-1}\times(w/P) \approx w/P$ for small η. Combining these expressions gives $d\omega_{rms}^2/dP \approx \omega_{rms}^2/P$ and $dA^2/dP \approx 3A^2/2P$. Finally, Section 3 gave $dg/dP = \nu_{3\mathrm{dB}}^{Er} / \nu_{3\mathrm{dB}} \times (2P)^{-1}$ in terms of the measured bandwidths. Putting this all together, one arrives at

#9471 - $15.00 USD Received 10 November 2005; revised 6 December 2005; accepted 13 December 2005
(C) 2005 OSA

$$\frac{df_r}{dP} = -f_r^2 \left\{ \overbrace{\beta_2 \frac{d\omega_\Delta}{dP}}^{\text{Spectral Shift}} + \overbrace{\frac{\omega_{rms}^2 \beta_3}{2P}}^{\text{TOD}} + \overbrace{\frac{\nu_{3\text{dB}}^{Er}}{2P\nu_{3\text{dB}}\Omega_g}}^{\text{Gain}} + \overbrace{\frac{3\mu A^2 \delta}{2P\omega_0}}^{\text{SS}} \right\}, \tag{4}$$

which is identical to the expression given in Ref. [6] except for the numerical pre-factor in the TOD and SS terms that differ because of the DM soliton scaling discussed above.

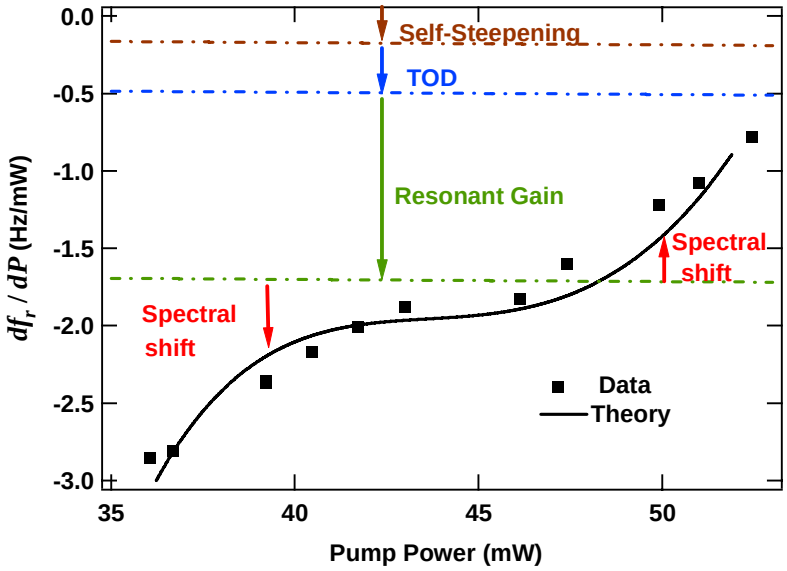

Fig. 7. The measured df_r/dP versus pump power. The strengths of the various contributions are shown, with the colors corresponding to the colored terms in Eq. (4). The sum of the effects yields the solid black line, to be compared to the experimental measurements (solid black squares).

Values of df_r/dP were measured as a function of pump power as described in Section 4. Figure 7 shows the values for one laser configuration. A comparison of these results to the predictions of Eq. (4) requires that we measure or estimate various physical quantities. Fortunately, most of the parameters can be measured from the output spectra of the laser (see Fig. 9 for some example spectra). Based on the position of the Kelly sidebands, we estimate β_2 = -0.06 ps^2 [22]. The measured spectral width gives ω_{rms}= (2π)0.85 THz. The previously discussed bandwidth measurement yields $\nu_{3\text{dB}}^{Er}/\nu_{3\text{dB}} \approx 0.1$. Based on the estimated recirculating power of 0.07 nJ and pulse full width half maximum of 230 fs, the peak intensity is A^2=0.3 kW as given earlier. Values for $d\omega_\Delta/dP$ were determined from the measured spectra versus power as discussed in much more detail in the next Section. Finally, using the estimated values of $\omega_0 \approx 2\pi c/1560$ nm $\beta_3 = 4.0\times10^{-4}$ ps^3, δ = 6 kW^{-1}, and $\Omega_g = (2\pi)$0.3 THz, we obtain the solid line in Fig. 7. Also seen in Fig. 7 are the individual contributions of each of the terms of Eq. (4). All the effects, except for spectral shifts to higher frequencies, cause a decrease in the repetition rate – in other words a slowing down of the pulse. For the fiber-laser system, the dominant effect comes from the resonant gain contribution and the spectral shifts. The magnitude of the resonant gain contribution will depend strongly on the nonlinear loss factor η, since it determines the gain change associated with a change in pump power. The magnitude of the spectral shift contribution will depend in part on the frequency-dependent loss of the cavity (as described in Section 6). Therefore, both of these dominant effects will have a magnitude that is dependent on the specifics of the actual laser system.

#9471 - $15.00 USD Received 10 November 2005; revised 6 December 2005; accepted 13 December 2005
(C) 2005 OSA

Other systems with higher circulating power or different values of η could exhibit different dominant effects. In general the identification of the main mechanism for pump-power control of the repetition frequency and offset frequency is complicated. The magnitude of each term should be estimated carefully, and competition between the terms can even lead to sign changes in the value of df_r/dP and df_{CEO}/dP.

6. Intensity-dependent spectral shifts

The importance of pump-induced spectral shifts was recognized in very early work [8] and its importance has been noted for both Ti:Sapphire [10] and fiber-laser based frequency combs [12]. The basic effect is quite simple; a shift in the spectrum causes a shift in the round trip time, $\omega_\Delta\beta_2$, due to the net cavity dispersion as in Eq. (3). In so much as ω_Δ and β_2 can be measured experimentally, the strength of this effect is easily calculated as in Eq. (4). However, given the apparent importance of this effect, it is worth considering what actually causes the pump-induced spectral shift.

The two effects of frequency-dependent loss and nonlinear frequency shifts can lead to a pump-induced frequency shift. In each case, a frequency-pulling effect is counteracted by the filtering effects of the gain profile. Figure 8 shows schematically the competing effects. The nonlinear component to the frequency shift, $\omega_{\Delta,NL}$, arises primarily from the well-known Raman self-frequency shift, although self-steepening can also contribute for a chirped pulse. The linear component, $\omega_{\Delta,L}$ arises from a slope to the cavity loss, $l_\omega = dl/d\omega$. Mathematically, [6]

$$\omega_{\Delta,NL} = \frac{-2A^2\delta}{5D_g(1+C^2)}\left(\tau_R + \mu\omega_0^{-1}C\right) \text{ and } \omega_{\Delta,L} = -\frac{l_\omega}{2D_g}, \tag{5}$$

where C is the pulse chirp and $D_g \sim 5000$ fs^2 is the second derivative of the power-broadened gain, *i.e.* the curvature of the gain as a function of frequency.

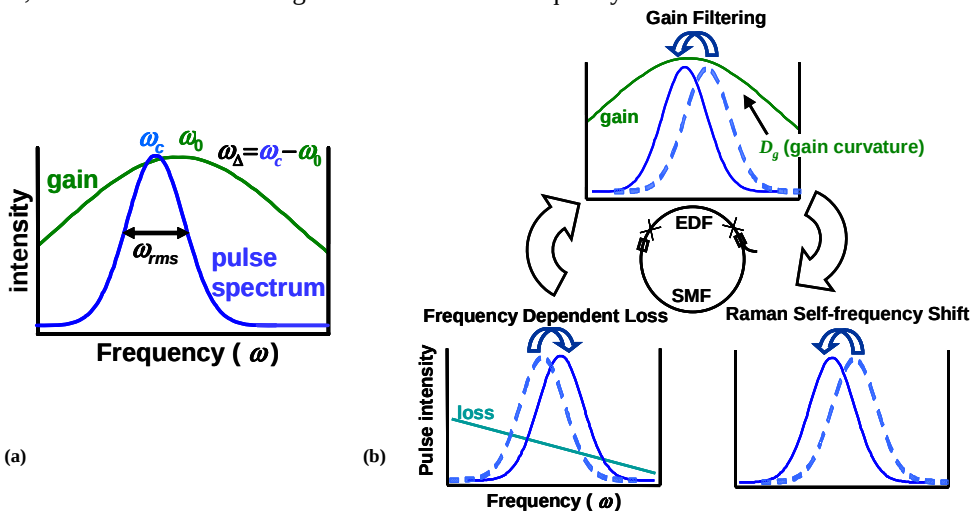

Fig. 8. (a) Definition of frequency terms: ω_0 is the gain peak, ω_c is the pulse spectral peak, ω_{rms} is the pulse spectral width, and $\omega_\Delta=\omega_c-\omega_0$. (b)Schematic showing the spectral shift effects following Ref. [6]. The pulse can shift higher or lower in frequency if there is a frequency dependent loss. It will shift lower in frequency due to the Raman self-frequency shift. In the EDF, it will shift back toward the gain peak at ω_0 due to gain filtering.

The gain filtering term, D_g, decreases with increasing pump power due to power-broadening. (This effect is more important than any increase in D_g due to the pump-induced gain increase

#9471 - $15.00 USD Received 10 November 2005; revised 6 December 2005; accepted 13 December 2005
(C) 2005 OSA

which is suppressed at small values of η.) Assuming that the highly power-broadened gain scales as $D_g \propto P^{-1}$, and using $A \propto w^{3/4}$, one can derive

$$\frac{d\omega_\Delta}{dP} = \left(\omega_{\Delta,NL} + \omega_{\Delta,L}\right)\frac{1}{P} + \frac{3\omega_{\Delta,NL}}{2w}\frac{dw}{dP}. \quad (6)$$

Previously, in deriving Eq. (4), we made the assumption that $dw/dP = w/P$ which, if used in Eq. (6), would predict a linear frequency shift with pump power. However, cw breakthrough is observed at higher pump power, which causes a reduction in dw/dP and so we retain dw/dP in Eq. (6). (This effect was ignored in Section 5 for simplicity but does effect the TOD and SS contributions at high P in Fig. 7). Note that both the pulse and cw components of the circulating power contribute to the power broadening of the gain.

Experimentally, the spectral shifts are challenging to measure since they are quite small. However, modern optical spectrum analyzers have remarkable resolution and very low drift over short times so that we are able to reliably measure small spectral shifts. Some example spectra are given in Fig. 9(a). Each spectrum was fit to a sech^2 shape after masking out the Kelly sidebands and any cw spike. Figure 9(b) shows the result for the center of the spectrum as a function of pump power. The solid line is a polynomial fit to the data.

The derivative of the polynomial fit of Fig. 9(b) gives $d\omega_\Delta/dP$ (Fig. 10) and is used in calculating df_r/dP using Eq. (4). This derivative should agree with the theoretical predictions from Eq. (6). From the same set of measured spectra, the integrated power excluding the cw peak provides a measure of the total pulse energy w. We find that dw/dP does indeed decrease at higher pump powers as more of the pump power is translated into cw laser power. Qualitatively, it is expected that the decrease in the spectral shift with larger pump power to result from competition between the nonlinear frequency shift and the linear frequency shift (if they have opposite signs). The decrease in dw/dP leads to an ever decreasing contribution from the nonlinear frequency shift. To be more quantitative, we fit the data in Fig. 10 to Eq. (6) using the measured dw/dP. The fit, shown as a dotted line in Fig. 10, gave the values for the frequency shifts of $\omega_{\Delta,NL}^{fit} = -3.1\times10^{-4}$ fs^{-1} and $\omega_{\Delta,L}^{fit} = 6.3\times10^{-4}$ fs^{-1}. These values compare reasonably well with the values of $\omega_{\Delta,NL}^{theory} = -7\times10^{-4}$ fs^{-1} and $\omega_{\Delta,L}^{theory} = 5\times10^{-4}$ fs^{-1} predicted from Eq. (5) using the experimentally measured l_ω= -5 fs and C=0, particularly considering nonzero chirp will only decrease $\omega_{\Delta,NL}^{theory}$. Finally, we note that in principle, l_ω is under experimental control and could be "tuned" to achieve a specific pump-induced spectral shift.

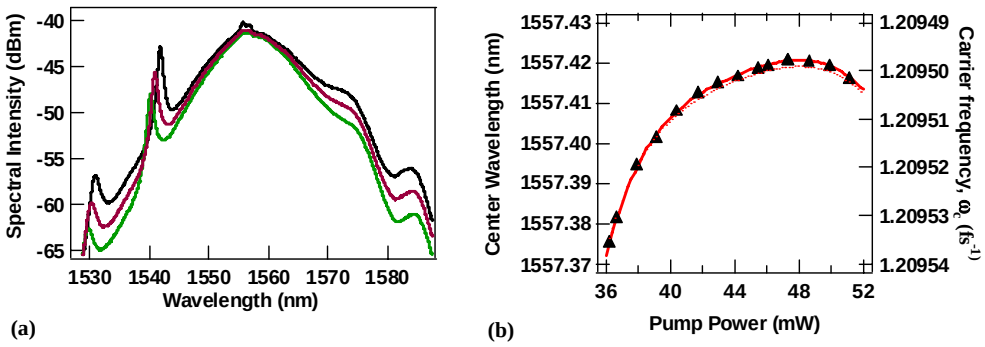

Fig. 9. (a) Example OSA spectra taken at pump powers (above threshold) of 38 mW (green), 43 mW (brown) and 50 mW (black). The peaks on the sides are Kelly sidebands. The bump in the center of the spectrum at high pump powers (black trace) is from cw breakthrough that occurs at higher pump powers. (b) Center of the spectrum from a fit to the OSA spectra as a function of pump power (triangles) and a polynomial fit (solid line).

#9471 - $15.00 USD Received 10 November 2005; revised 6 December 2005; accepted 13 December 2005
(C) 2005 OSA

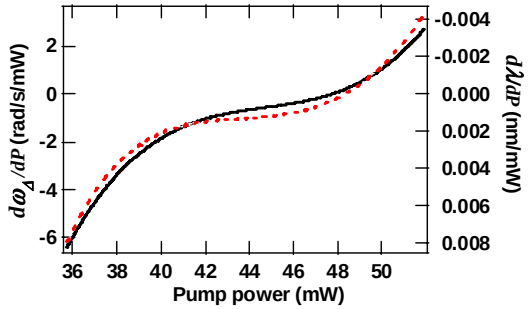

Fig. 10. Pump-induced spectral shifts: The solid line is the "measured" values taken as the derivative of the polynomial fit to the data in Fig. 9(b). These data are used in calculating the spectral-shift contribution to df_r/dP given in Fig. 7. The dashed line is a fit to the data using the theoretical expression Eq. (6) and the measured dw/dP.

7. Summary

We have presented a detailed comparison of experiment and theory for the pump-power control of a frequency comb output by a fiber laser. Based on this comparison, we can make a number of conclusions. First, for systems that use pump power to phase-lock f_{CEO}, the bandwidth of the phase-lock will be limited by the response bandwidth of the laser. We find this response bandwidth will always exceed that of the gain medium by an amount that is related to the laser stability. The greater this response bandwidth exceeds the Er gain response, the less stable a pulse train, as confirmed by the f_{CEO} beat note width. Second, the response of f_{CEO} and f_r are consistent with a theory that includes saturation of the self-amplitude modulation, resonant gain contribution, spectral shifts, third-order dispersion, the Raman effect, self-phase modulation, and self-steepening. For our system, the pump-induced change in f_r is dominated by the resonant gain contribution and by the spectral shifts. Moreover, these pump-induced spectral shifts can be explained by a combination of linear and nonlinear frequency pulling effects coupled with gain filtering. Finally, despite this complexity, the pump-induced shift in f_{CEO} and f_r are related by a simple linear relationship that is easily measured using frequency counters.

Acknowledgments

We acknowledge J. W. Nicholson, K. Feder, and P. S. Westbrook for the highly nonlinear fiber and John McFerran for useful discussions.

#9471 - $15.00 USD Received 10 November 2005; revised 6 December 2005; accepted 13 December 2005
(C) 2005 OSA